

Global fits to $b \rightarrow s\ell\ell$ data

Flavour@TH 2023 – 11/05/2023

Méril Reboud

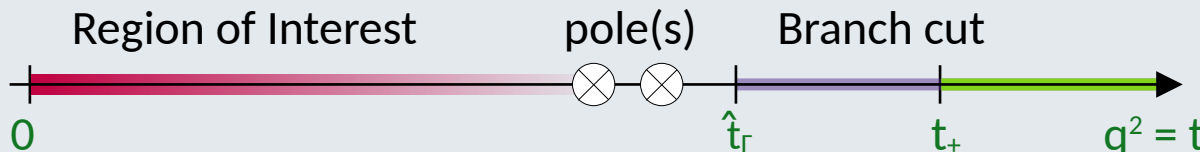
Based on:

- Gubernari, van Dyk, JV 2011.09813
- Gubernari, Reboud, van Dyk, JV 2206.03797
- Ahmis, Bordone, Reboud 2208.08937
- Gubernari, Reboud, van Dyk, JV [2305.06301](#)

Introduction

- Previously in Flavour@TH 2023:

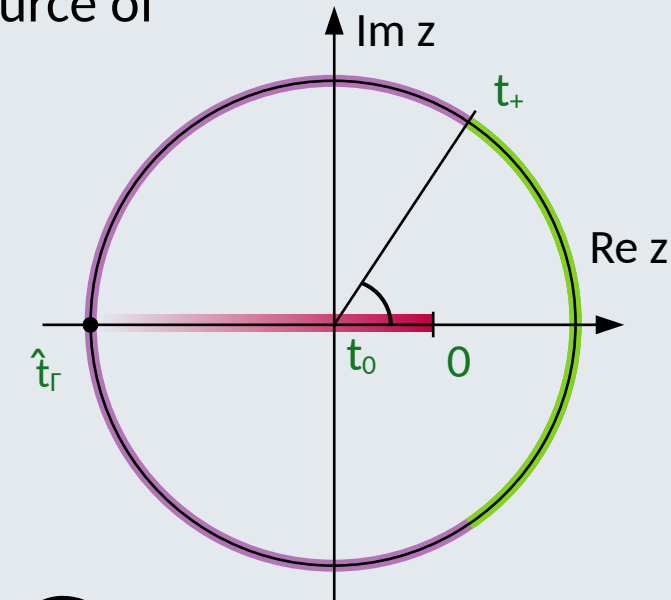
- Local and non-local form factors are the main source of uncertainties in $b \rightarrow s\ell\ell$ decays
- Both follow the same analytic structure:



- The GRvDV parametrization diagonalizes the dispersive bounds:

$$\hat{z}(q^2) = \frac{\sqrt{\hat{t}_\Gamma - q^2} - \sqrt{\hat{t}_\Gamma}}{\sqrt{\hat{t}_\Gamma - q^2} + \sqrt{\hat{t}_\Gamma}}$$

$$\hat{\mathcal{H}}(\hat{z}) = \sum_{n=0}^{\infty} \beta_n p_n(\hat{z})$$



Orthonormal
polynomials of the arc
of the unit circle

Introduction and Outline

- I will cover three types of global $b \rightarrow s\ell\ell$ fits:
 - The fit of the local form factors using dispersive bounds
 - The fit of the non local contributions charm loops
 - The fit of WET coefficients based on experimental data
- Given the discussion we had so far [esp. during Jonathan's, Paolo's and Martin's talk], I will start with discussing the parametrization in practice with $\Lambda_b \rightarrow \Lambda^*\ell\ell$

I. The method in practice

Example with $\Lambda_b \rightarrow \Lambda(1520) \ell\ell$

- Inputs:
 - LQCD estimates at $q^2 = 16.3$ and 16.5 GeV^2 [Meinel, Rendon '21]
 - no LCSR available
→ use (loose) **SCET relations** [Descotes-Genon, M. Novoa-Brunet '19]

$$\begin{aligned} f_{\perp'}(0) &= 0 \pm 0.2, & g_{\perp'}(0) &= 0 \pm 0.2, & h_{\perp'}(0) &= 0 \pm 0.2, \\ \tilde{h}_{\perp'}(0) &= 0 \pm 0.2, & f_+(0)/f_{\perp}(0) &= 1 \pm 0.2, & f_{\perp}(0)/g_0(0) &= 1 \pm 0.2, \\ g_{\perp}(0)/g_+(0) &= 1 \pm 0.2, & h_+(0)/h_{\perp}(0) &= 1 \pm 0.2, & f_+(0)/h_+(0) &= 1 \pm 0.2, \end{aligned}$$

$O(\alpha_s/\pi, \Lambda_{\text{QCD}}/m_b)$

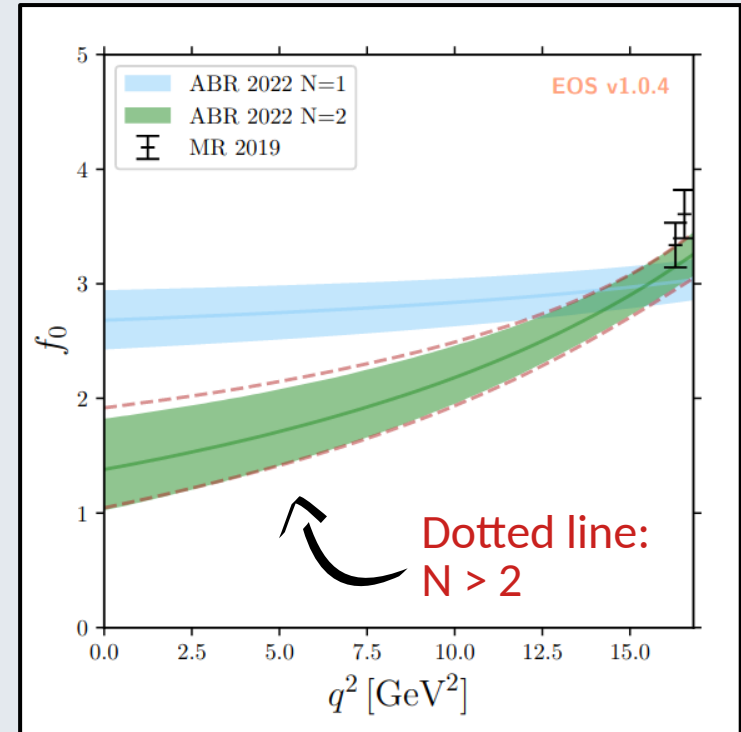
- 14 form factors: **17 parameters ($N = 1$)**, **31 parameters ($N = 2$)**
21 LQCD inputs + 9 SCET relations: **30 constraints**

 $2 * 14 - 7$ endpoint relations at q^2_{\max}

Example with $\Lambda_b \rightarrow \Lambda(1520)\ell\ell$



- $N = 1$ does not give a good fit (p value ~ 0)
- Use an **under-constrained fit** ($N > 1$) and allows for saturation of the dispersive bound
 - The uncertainties are truncation order independent: increasing the order does not change their size
- Same conclusions were found for $\Lambda_b \rightarrow \Lambda$ form factors [Blake, Meinel, Rahimi, van Dyk '22]

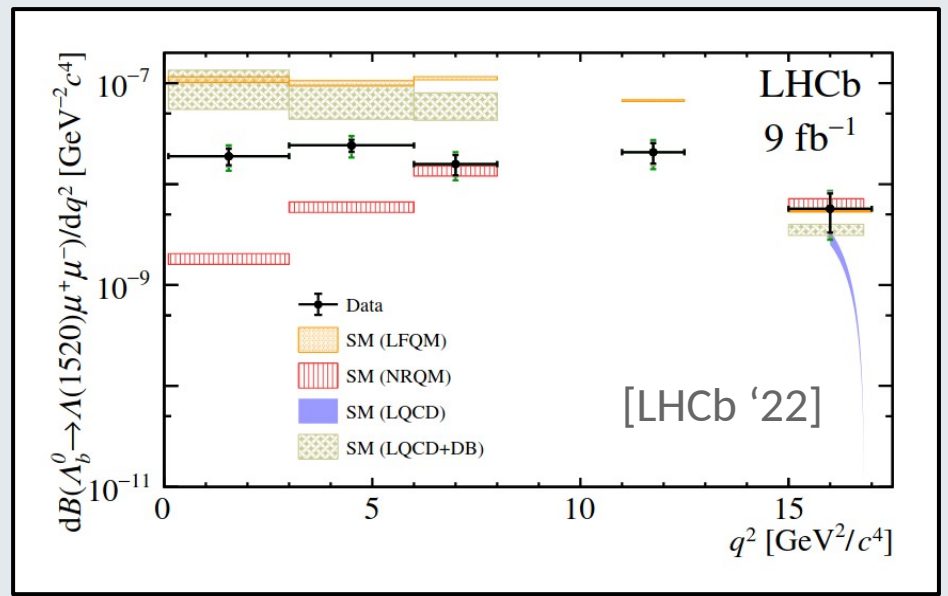
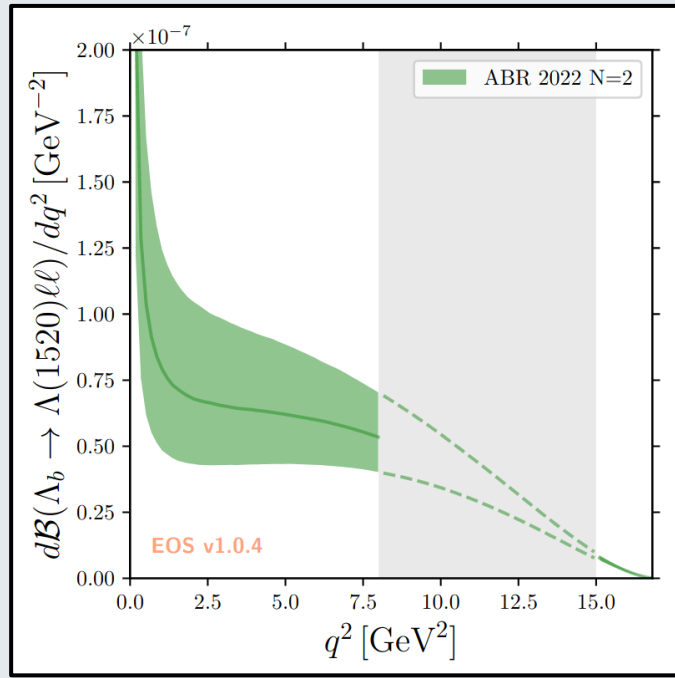


[Ahmisi, MR, Bordone '22]

Phenomenology



- Uncertainties are large but **under control** and **systematically improvable**
- LHCb analysis confirmed the usual $b \rightarrow s\ell\ell$ tension at low q^2

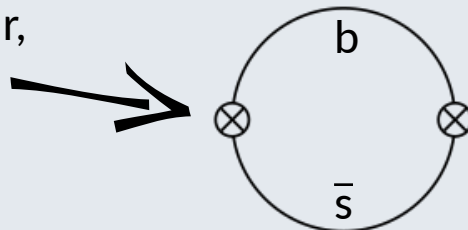


II. Improved dispersive bounds

Correlator and Helicities

- **Main idea:** Compute the inclusive $e^+e^- \rightarrow \bar{b}s$ cross-section and relate it to the form factors [Bharucha, Feldmann, Wick '10]

Insertion of a scalar,
vector or tensor
current



+ other diagrams: loops,
quark and gluon
condensates...

- Usually, the correlator $\Pi_{\Gamma}^{\mu\nu}(q) \equiv i \int d^4x e^{iq \cdot x} \langle 0 | \mathcal{T} \left\{ J_{\Gamma}^{\mu}(x) J_{\Gamma}^{\dagger,\nu}(0) \right\} | 0 \rangle$

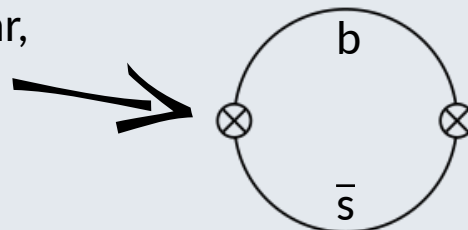
is decomposed as:

$$\Pi_{\Gamma}^{\mu\nu}(q) \equiv \frac{q^{\mu}q^{\nu}}{q^2} \Pi_{\Gamma}^{(J=0)} + \frac{1}{D-1} \left(\frac{q^{\mu}q^{\nu}}{q^2} - g^{\mu\nu} \right) \Pi_{\Gamma}^{(J=1)}$$

Correlator and Helicities

- **Main idea:** Compute the inclusive $e^+e^- \rightarrow \bar{b}s$ cross-section and relate it to the form factors [Bharucha, Feldmann, Wick '10]

Insertion of a scalar,
vector or tensor
current



+ other diagrams: loops,
quark and gluon
condensates...

- We suggest the more generic decomposition:

$$\Pi_{\Gamma}^{\mu\nu}(q) \equiv \sum_{\lambda,\lambda'} \epsilon^{\mu}(\lambda) \epsilon^{\nu*}(\lambda') \Pi_{\Gamma}^{(\lambda,\lambda')}(q^2)$$

Two wavy lines representing polarization vectors, with arrows indicating their direction. They are positioned below the equation, with a brace underneath them.

Polarization vectors

Correlator and Helicities

- **Main advantage:**

- The OPE calculation is independent of the helicities:

$$\Pi_{\Gamma}^{(J=1)}|_{\text{OPE}} = \Pi_{\Gamma}^{(0)}|_{\text{OPE}} = \Pi_{\Gamma}^{(\parallel)}|_{\text{OPE}} = \Pi_{\Gamma}^{(\perp)}|_{\text{OPE}}$$

→ The calculation of Ref. [Bharucha, Feldmann, Wick '10] still applies!

- Remove spurious correlations between form factors:
 - e.g. A_1 and A_{12} now fulfill different bounds
 - decorrelate completely $B \rightarrow K$ from $(B \rightarrow K^*, B_s \rightarrow \varphi)$

Correlator and Helicities

- In equations:

- This is the bound used in the literature:

$$\chi_A^{(J=1)}|_{BK^*} = \frac{\eta^{B \rightarrow K^*}}{24\pi^2} \int_{(M_B+M_{K^*})^2}^{\infty} ds \frac{\lambda_{\text{kin}}^{1/2}}{s^2(s-Q^2)^3} \left[s(M_B+M_{K^*})^2 |A_1^{B \rightarrow K^*}|^2 + 32 M_B^2 M_{K^*}^2 |A_{12}^{B \rightarrow K^*}|^2 \right]$$

- And this is what we propose:

$$\chi_A^{(0)}|_{\bar{B}K^*} = \frac{\eta^{B \rightarrow K^*}}{\pi^2} \int_{(M_B+M_{K^*})^2}^{\infty} ds \frac{\lambda_{\text{kin}}^{1/2}}{s^2(s-Q^2)^3} 4 M_B^2 M_{K^*}^2 |A_{12}^{B \rightarrow K^*}|^2,$$

$$\chi_A^{(\parallel)}|_{\bar{B}K^*} = \frac{\eta^{B \rightarrow K^*}}{8\pi^2} \int_{(M_B+M_{K^*})^2}^{\infty} ds \frac{\lambda_{\text{kin}}^{1/2}}{s^2(s-Q^2)^3} s(M_B+M_{K^*})^2 |A_1^{B \rightarrow K^*}|^2,$$

Local form factors fit

- With this framework we perform a **combined fit** of $B \rightarrow K$, $B \rightarrow K^*$ and $B_s \rightarrow \varphi$ LCSR and lattice QCD inputs:
 - $B \rightarrow K$:
 - [HPQCD '13 and '22; FNAL/MILC '17]
 - ([Khodjamiriam, Rusov '17]) → large uncertainties, not used in the fit
 - $B \rightarrow K^*$:
 - [Horgan, Liu, Meinel, Wingate '15]
 - [Gubernari, Kokulu, van Dyk '18] (B-meson LCSRs)
 - $B_s \rightarrow \varphi$:
 - [Horgan, Liu, Meinel, Wingate '15]
 - [Gubernari, van Dyk, Virto '20] (B-meson LCSRs)
- Baryonic decays should be added, but there are currently only few constraints

- Bayesian analysis using EOS
- Implementation of the dispersive bound:

$$-2 \log P(r) = \begin{cases} 0 & \text{if } r < 1 , \\ \frac{(r-1)^2}{\sigma^2} & \text{otherwise ,} \end{cases}$$



10% uncertainty on the OPE calculation
[Bharucha, Feldmann, Wick '10]

- To many constraint to perform an under-constrained fit
→ **Stability criterion:** truncate the series expansion to $N = 2, 3, 4$ and compare the form factor uncertainties

- All the samples are considered to be **correlated only via the dispersive bounds**
 - Since $B \rightarrow K$ and $(B \rightarrow K^*, B_s \rightarrow \varphi)$ are decoupled, we perform **3 separated fits**
 - $B \rightarrow K^*$ and $B_s \rightarrow \varphi$ samples are combined with a weighting procedure:

$$w(r_{\Gamma,\lambda}^{B \rightarrow K^*}) = \int dr p_{\Gamma,\lambda}^{B_s \rightarrow \phi}(r) \times P(\text{dispersive bound for } \Gamma, \lambda | r_{\Gamma,\lambda}^{1\text{pt}} + r_{\Gamma,\lambda}^{B \rightarrow K^*} + r)$$

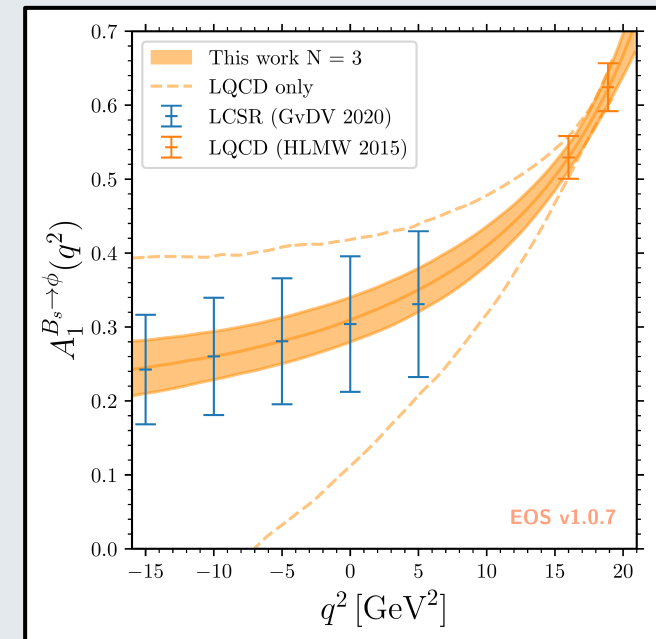
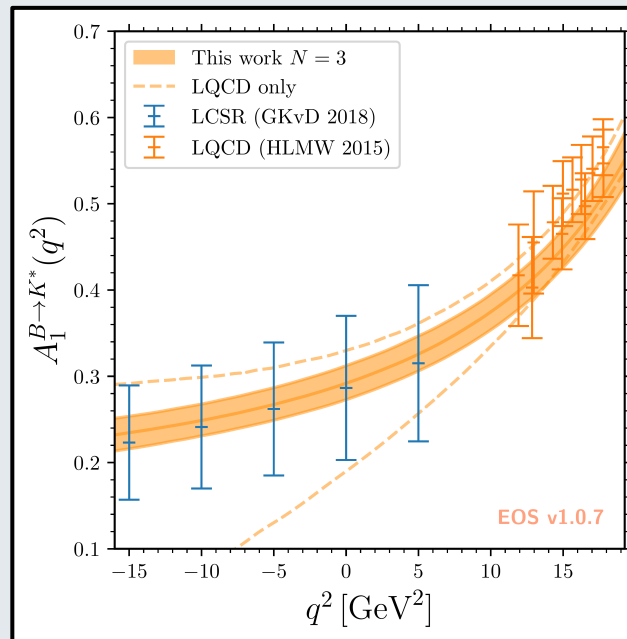
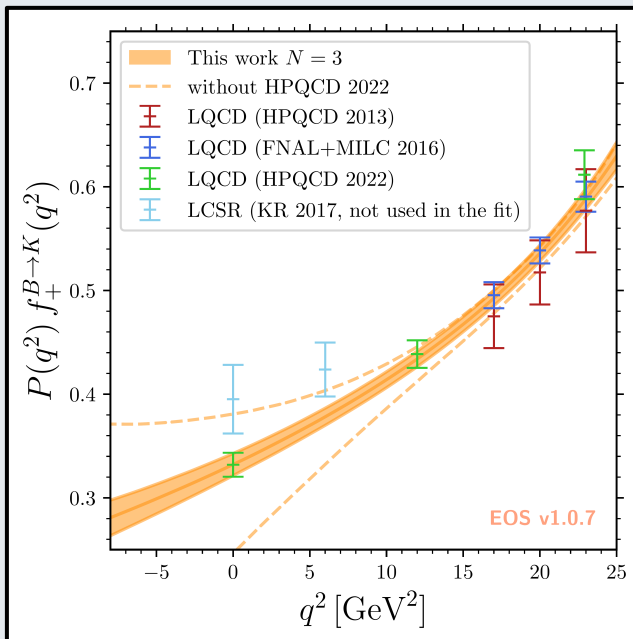
Current-specific weight

$$w^{B \rightarrow K^*} = \prod w(r_{\Gamma,\lambda}^{B \rightarrow K^*})$$

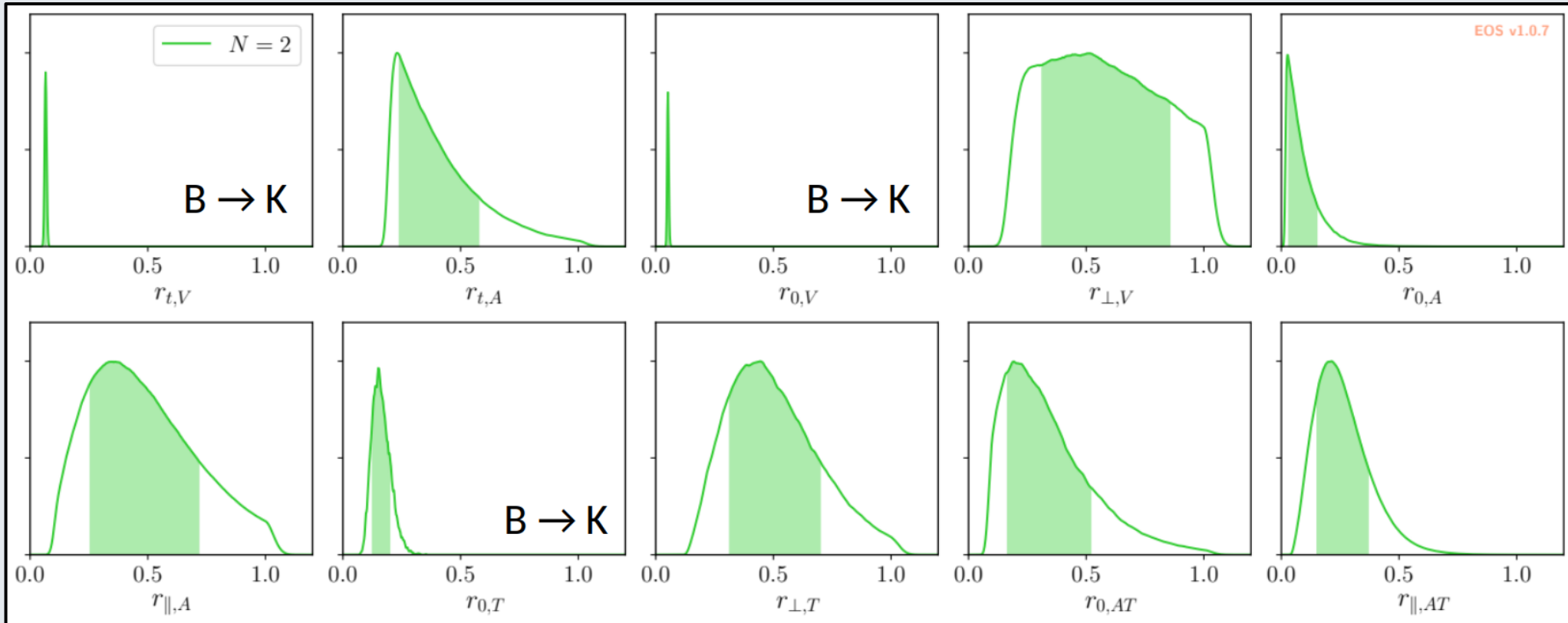
Results

Main conclusions:

- Fits are very good already at $N = 2$ (p -values $> 77\%$)
- LCSR and LQCD combine nicely and still dominate the uncertainties
- Progresses in LQCD will eventually make LCSR irrelevant (?)

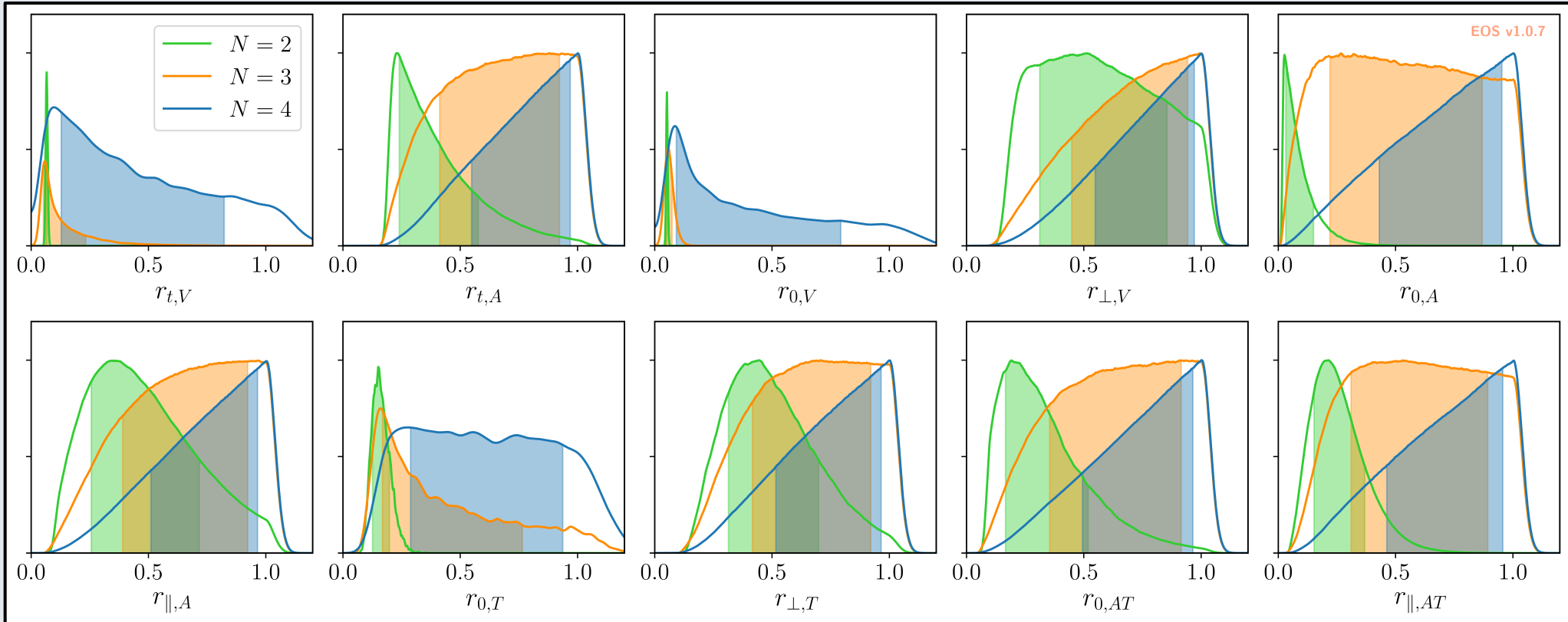


Saturations



- Saturations are small for $N = 2$, in agreement with [Bharucha, Feldmann, Wick '10]

Saturations

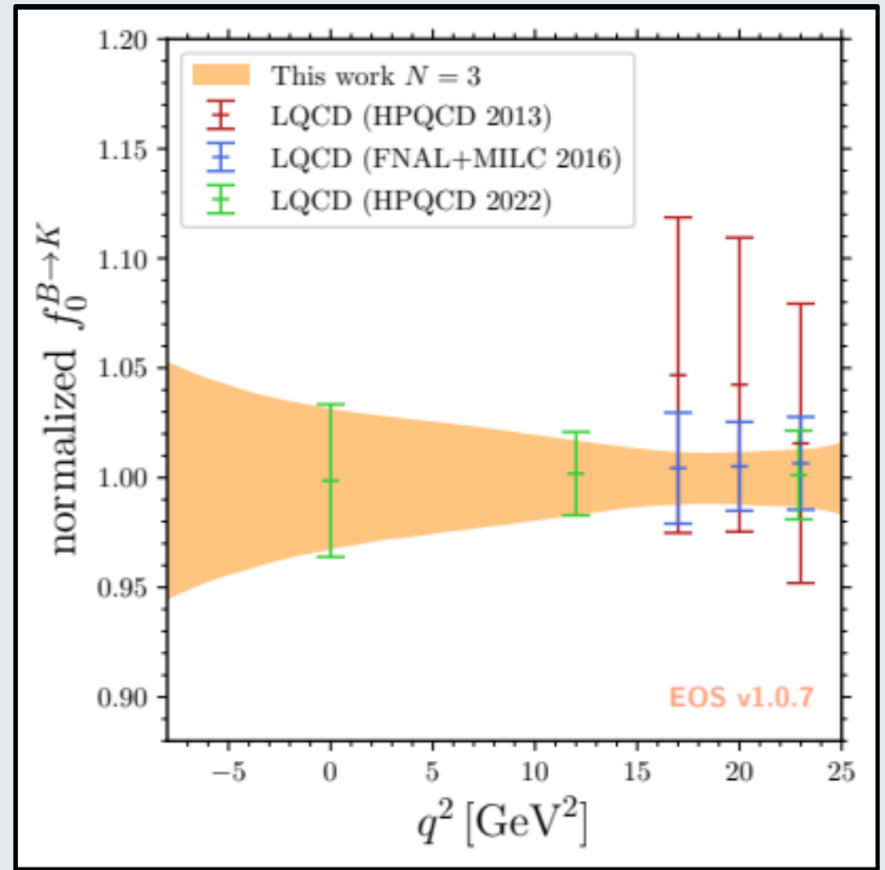


- The low saturations in $r_{t,V}$ and $r_{0,V}$ are probably due to large contributions in the baryonic decays, as discussed in the first part of this talk

Comparison plots



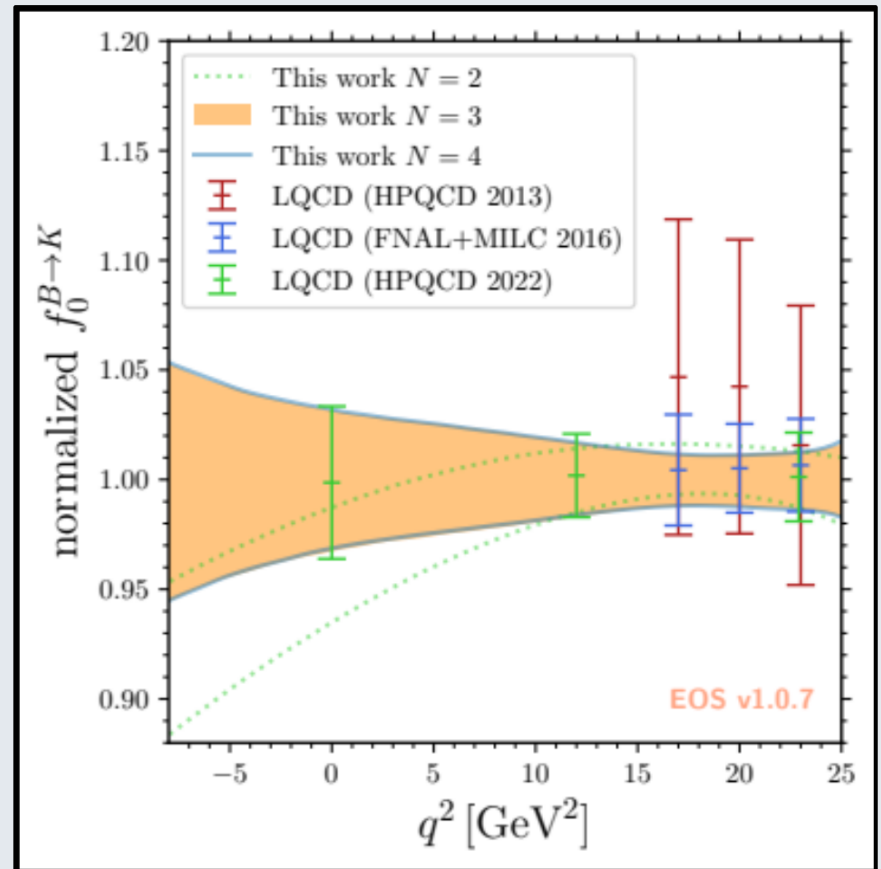
- For comparison purposes I normalize the form factors to our $N = 3$ best-fit point
- Uncertainties for $B \rightarrow K$ are now well below 5% in the physical region



Comparison plots



- For comparison purposes I normalize the form factors to our $N = 3$ best-fit point
- Uncertainties for $B \rightarrow K$ are now well below 5% in the physical region
- We compare the different values of the truncation order N

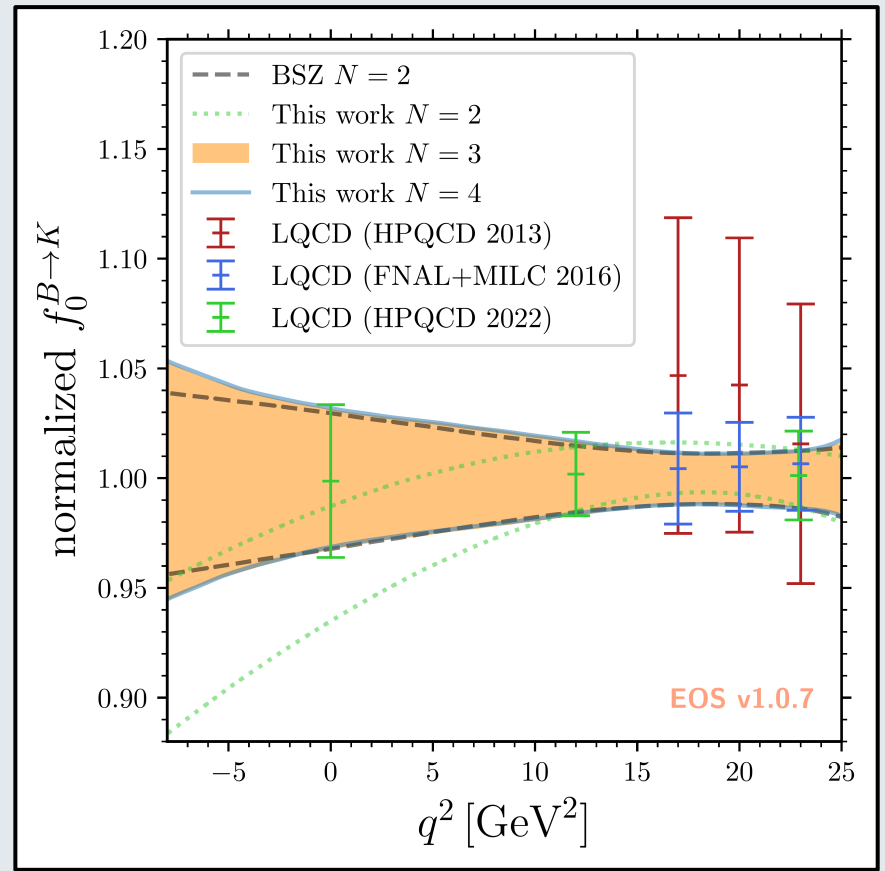


Comparison plots



- For comparison purposes I normalize the form factors to our $N = 3$ best-fit point
- Uncertainties for $B \rightarrow K$ are now well below 5% in the physical region
- We compare the different values of the truncation order N
- I also add the result of a usual Simplified Series Expansion à la [Bharucha, Feldmann, Wick '10; Bharucha, Straub, Zwicky '15]

$$f(t) = \frac{1}{P(t)} \sum_k \tilde{\alpha}_k z^k(t, t_0)$$

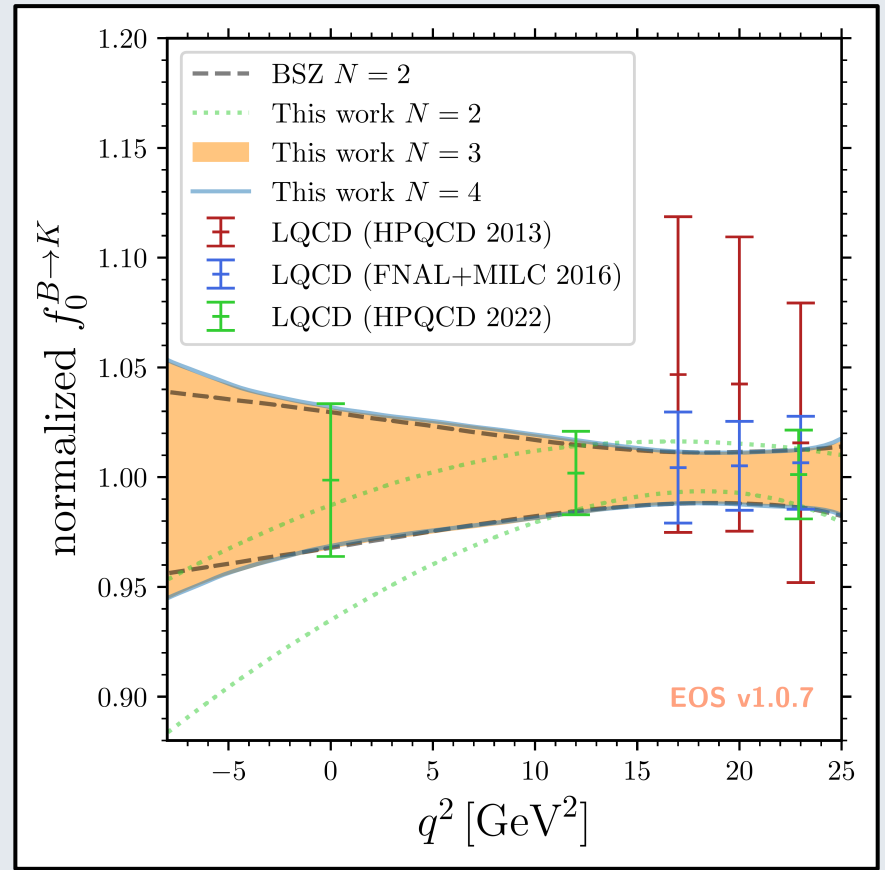


Generic result

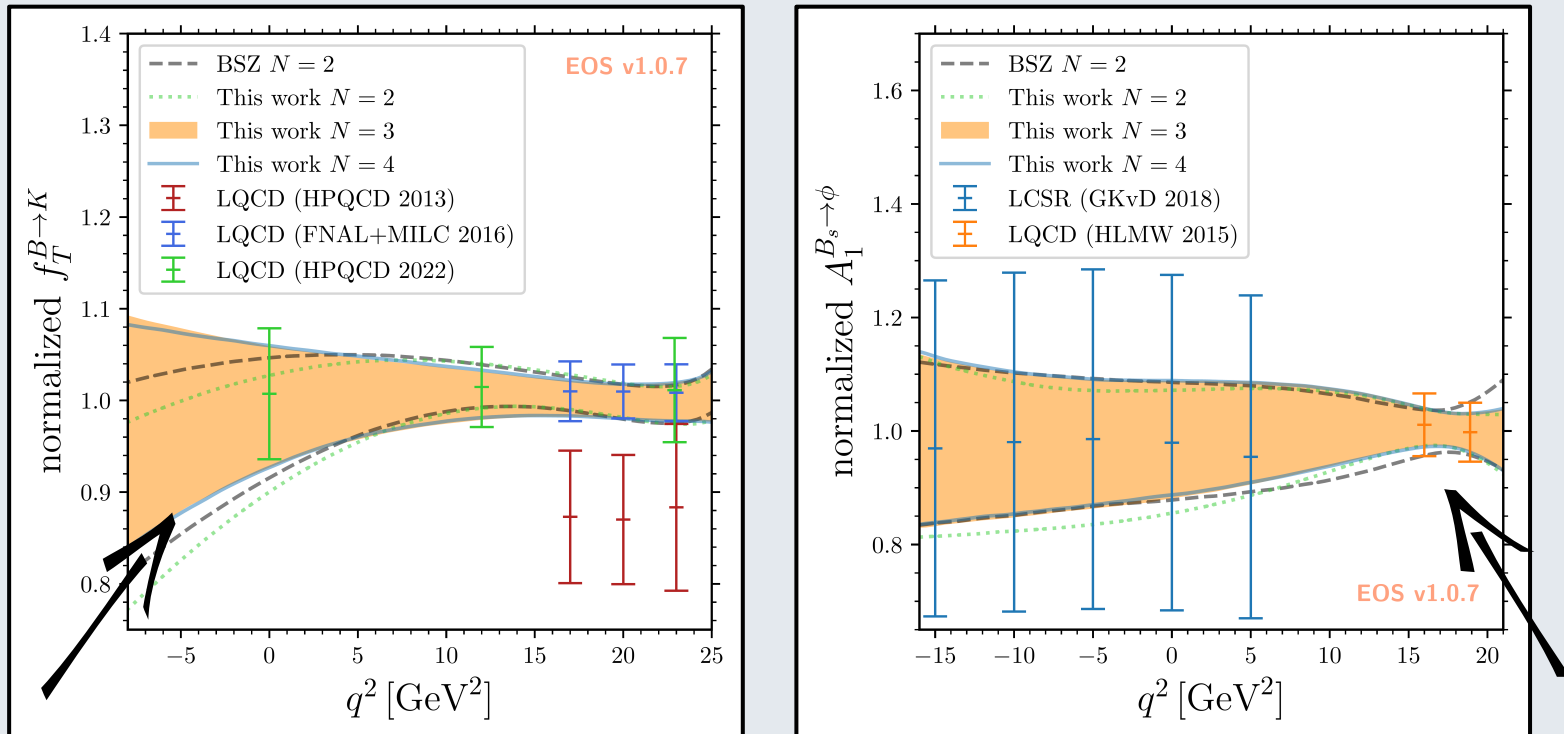


This is the generic result, namely:

- $N = 2$ shows a peculiar behaviour
- For $N > 2$ the uncertainties are stable
- BSZ is a good approximation in the physical range, but underestimates the uncertainties at negative q^2



Specific cases

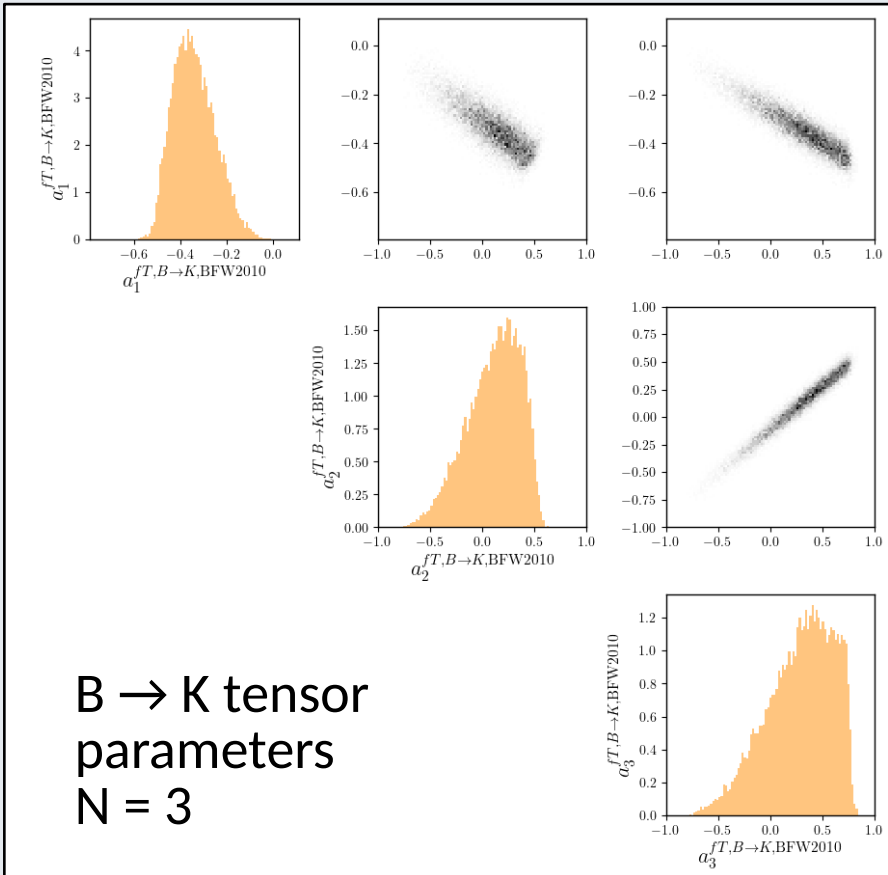


- The dispersive bounds stabilizes regions of the phase space with few theory constraints
- This is particularly useful at negative q^2 to estimate the non-local form factors

Gaussian and non-Gaussian behaviours



- For $N = 2$, the bounds are not saturated and the parameters follow Gaussian distributions to a good approximation (perplexities > 95%)
- Already at $N = 3$, distortions of the distribution are clearly visible



Where to find our results



- All the plots are available here: <https://doi.org/10.5281/zenodo.7919635>
- We also added
 - the updated posterior distributions for $N = 2$ in our parametrization and using a SSE as YAML files
 - All the tools/documentation to reproduce our results
- These results are also available in **EOS v1.0.7**:
 - [/eos/constraints/B-to-P-P-form-factors.yaml](#)
 - [/eos/constraints/B-to-P-P-form-factors.yaml](#)

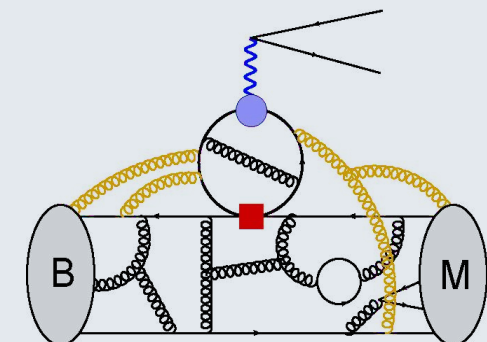
III. Parametrization of non-local form factors

→ I will stick to the conclusions of our paper and defer all discussion to this afternoon's session

Non-local form factors

$$\mathcal{A}_\lambda^{L,R}(B \rightarrow M_\lambda \ell \ell) = \mathcal{N}_\lambda \left\{ (C_9 \mp C_{10}) \mathcal{F}_\lambda(q^2) + \frac{2m_b M_B}{q^2} \left[C_7 \mathcal{F}_\lambda^T(q^2) - 16\pi^2 \frac{M_B}{m_b} \mathcal{H}_\lambda(q^2) \right] \right\}$$

$$\mathcal{H}_\mu(k, q) = i \int d^4x e^{iq \cdot x} \langle \bar{M}(k) | T\{\mathcal{J}_\mu^{\text{em}}(x), \mathcal{C}_i \mathcal{O}_i\} | \bar{B}(q+k) \rangle$$

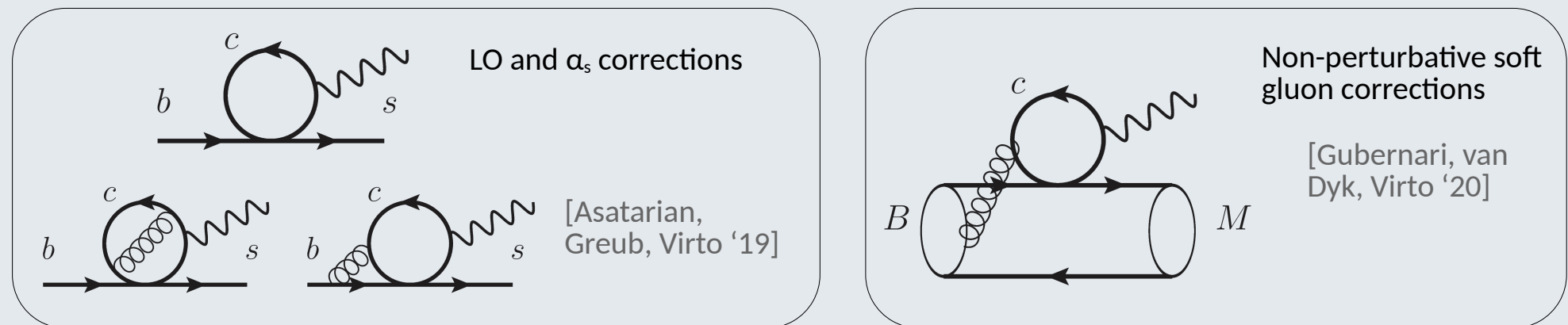


- Problematic because **they can mimic a BSM signal!**
 - \mathcal{H}_λ can be interpreted as a shift to C_9 and C_7
 - This shift is lepton-flavour universal (as now seen in the data)
- Notably **harder to estimate**, no lattice computation so far
- **Different parametrizations** are suggested

Theory inputs

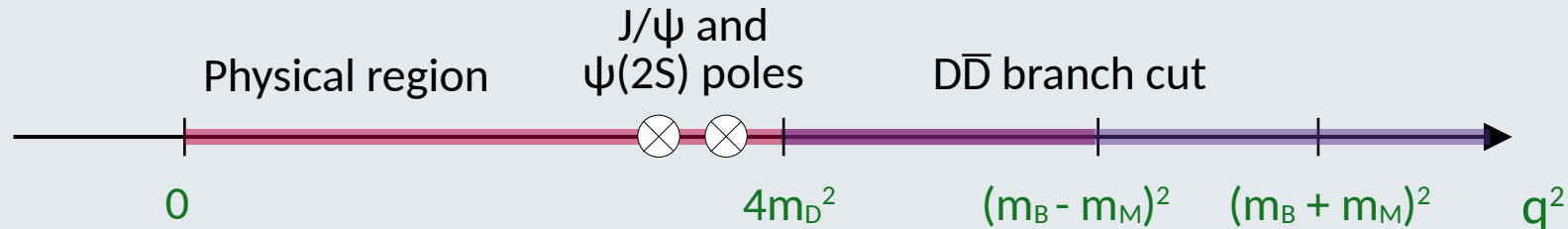
\mathcal{H}_λ can still be calculated in two kinematics regions:

- **Local OPE** $|q|^2 \gtrsim m_b^2$ [Grinstein, Piryol '04; Beylich, Buchalla, Feldmann '11]
- **Light Cone OPE** $q^2 \ll 4m_c^2$ [Khodjamirian, Mannel, Pivovarov, Wang '10]



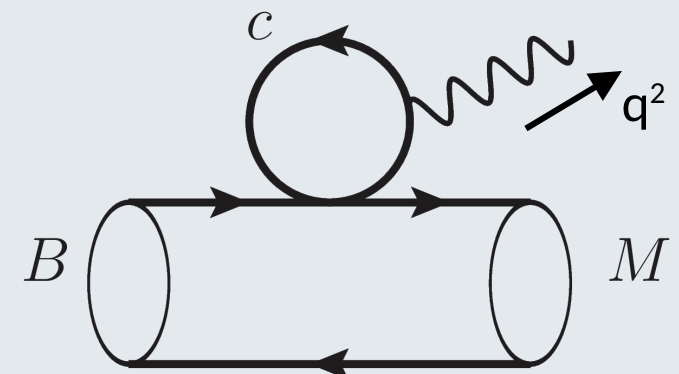
Analyticity properties

$$\mathcal{H}_\mu(k, q) = i \int d^4x e^{iq \cdot x} \langle \bar{M}(k) | T\{\mathcal{J}_\mu^{\text{em}}(x), \mathcal{C}_i \mathcal{O}_i\} | \bar{B}(q+k) \rangle$$



Analyticity properties of the Q_c dependent part:

- Poles due to **charmonium state**
- **Branch cut** in the physical range due to on-shell D meson production: $B \rightarrow M D\bar{D}$
- The branch cut in k^2 makes the coefficients of the z-expansion **complex-valued**



Parametrization of the charm loop

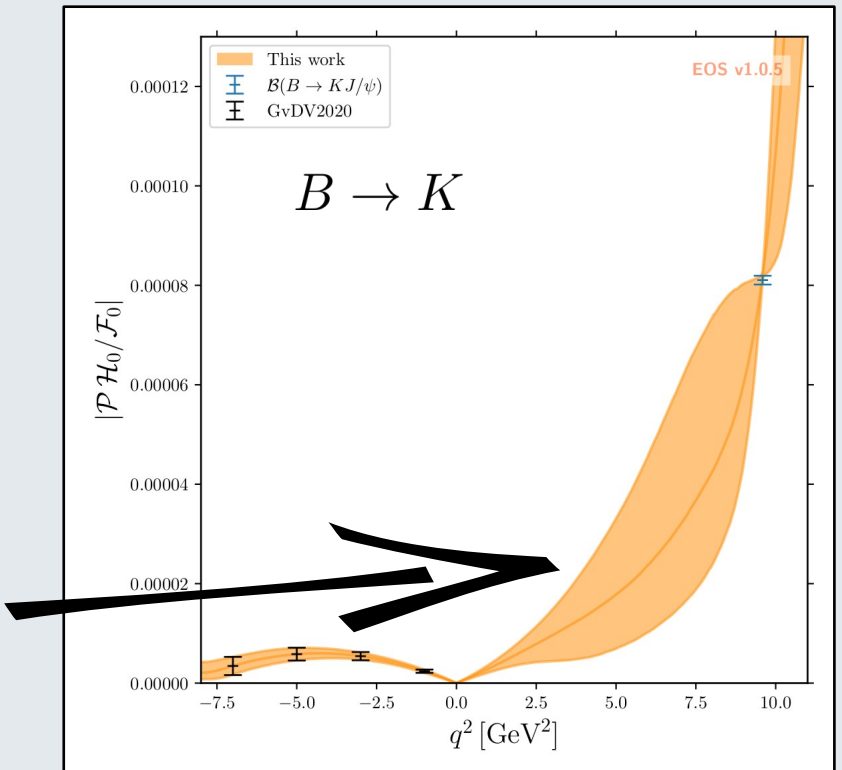


- Still focusing on $B \rightarrow K$, $B \rightarrow K^*$ and $B_s \rightarrow \varphi$

Inputs:

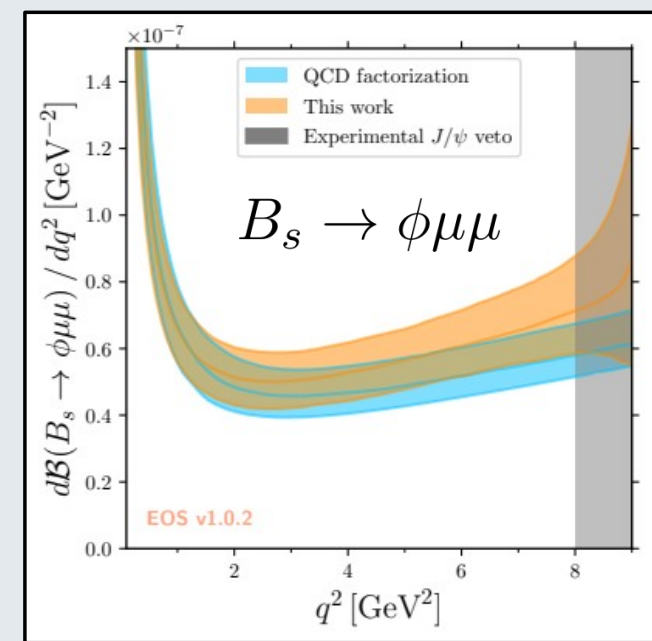
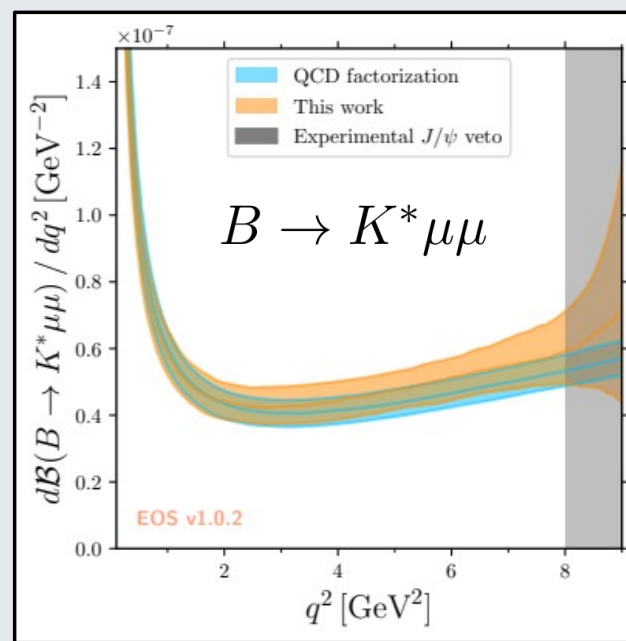
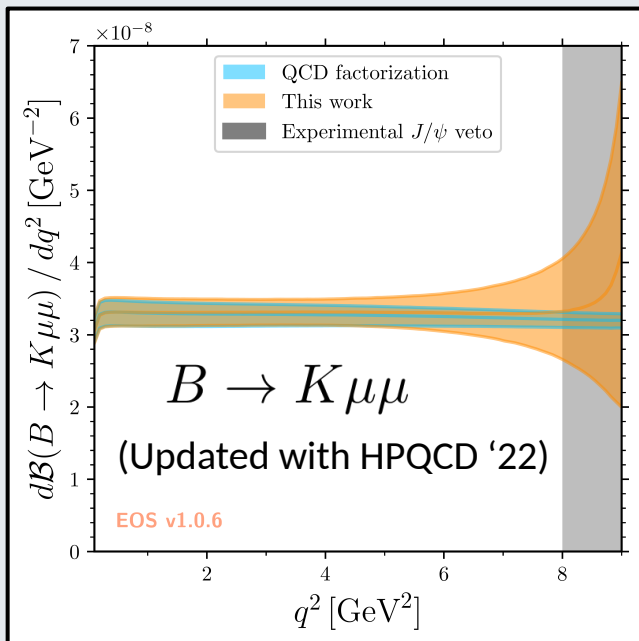
- 4 theory point at negative q^2 from the **light cone OPE**
 - Experimental results at the J/ψ (we keep $\psi(2S)$ for future work)
- Use again an under-constrained fit ($N = 5$) and allows for saturation of the dispersive bound
 - The uncertainties are **truncation order independent**, increasing the expansion order does not change their size
 - All p-values are larger than 11%

[Gubernari, MR, van Dyk, Virto '22]



SM predictions

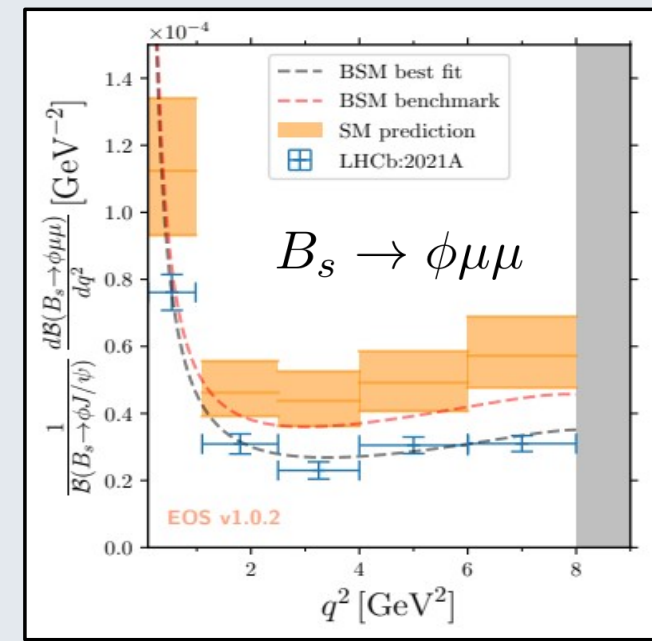
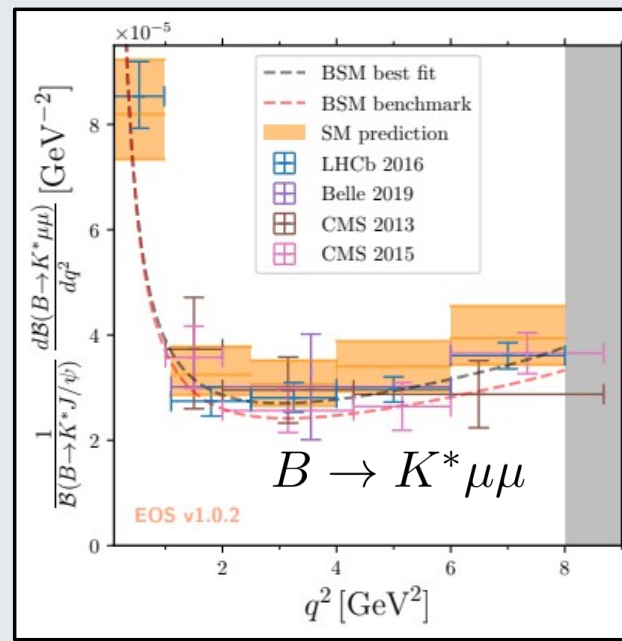
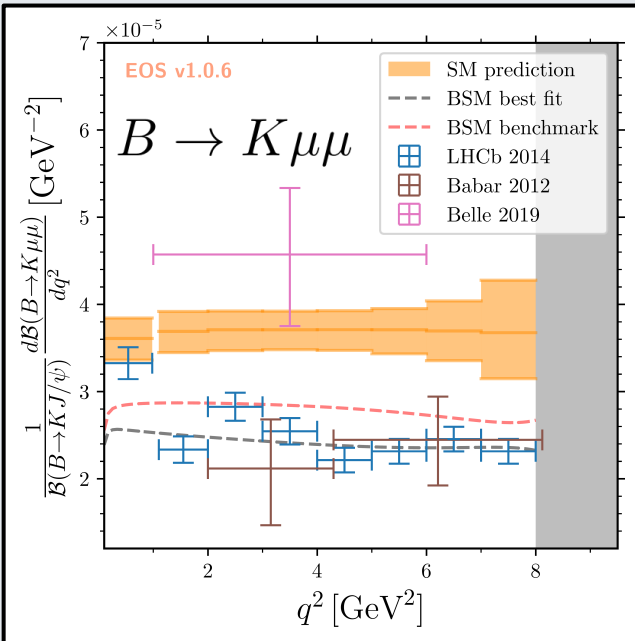
- Good overall agreement with previous theoretical approaches [Beneke, Feldman, Seidel '01 & '04]
 - Small deviation in the slope of $B_s \rightarrow \phi \mu \mu$
- Larger but controlled uncertainties especially near the J/ψ
 - The approach is **systematically improvable** (new channels, $\psi(2S)$ data...)



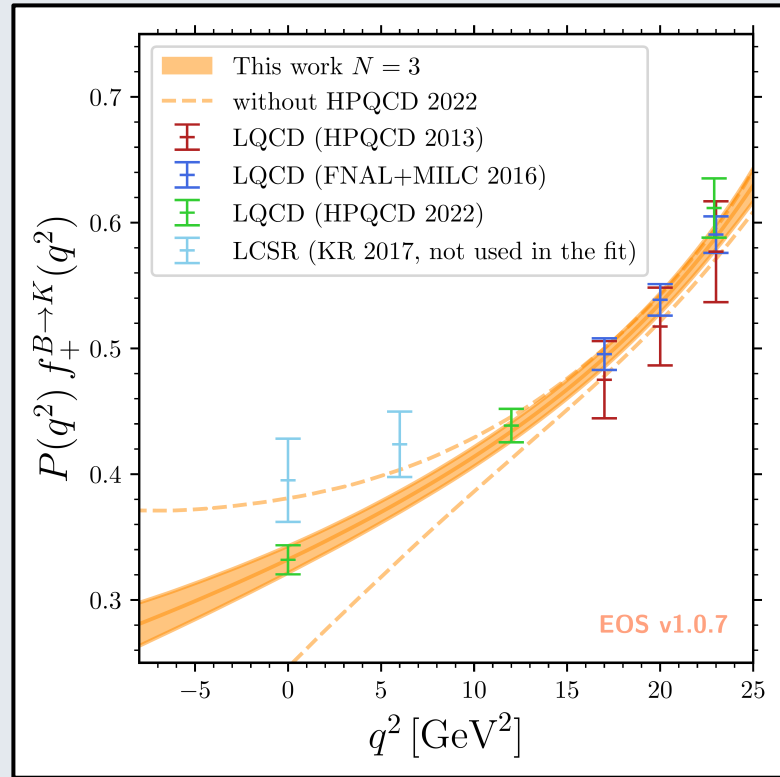
Comparison with data

- Conservatively accounting for the non-local form factors does not solve the $b \rightarrow s\mu\mu$ anomalies
- The largest source of theoretical uncertainty at low q^2 still comes from local form factors

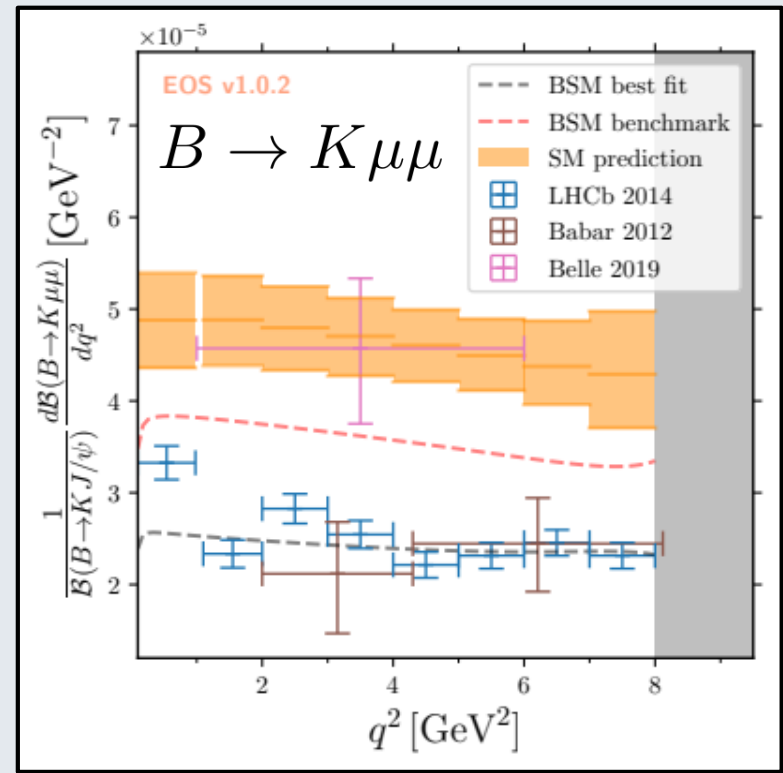
Experimental results:
 [Babar: 1204.3933; Belle: 1908.01848, 1904.02440; ATLAS: 1805.04000, CMS: 1308.3409, 1507.08126, 2010.13968, LHCb: 1403.8044, 2012.13241, 2003.04831, 1606.04731, 2107.13428]



Effect of HPQCD 2022

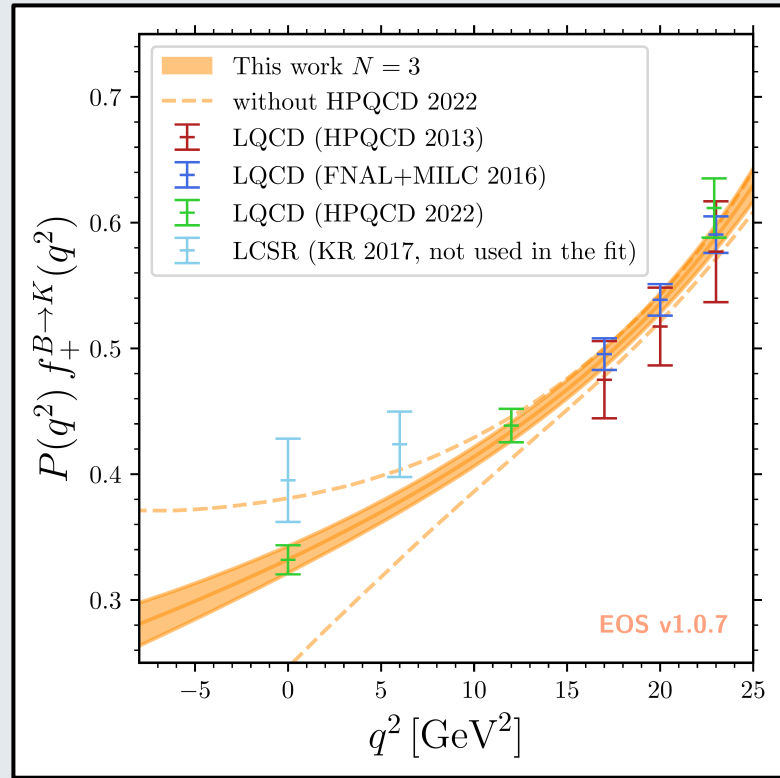


With Khodjamirian-Rusov 2017

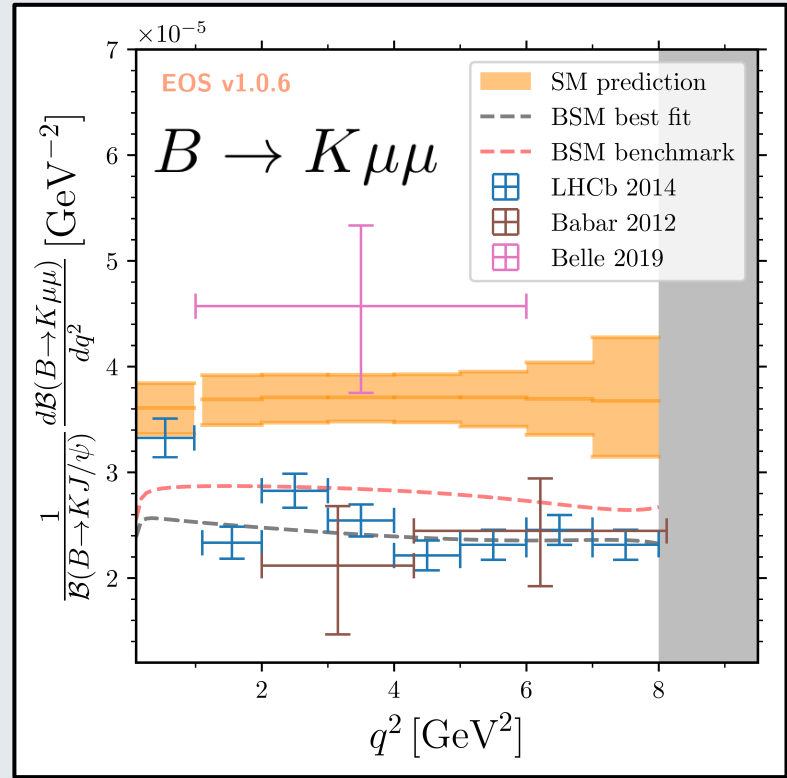


[Gubernari, MR, van Dyk, Virto '22]

Effect of HPQCD 2022



With HPQCD 2022

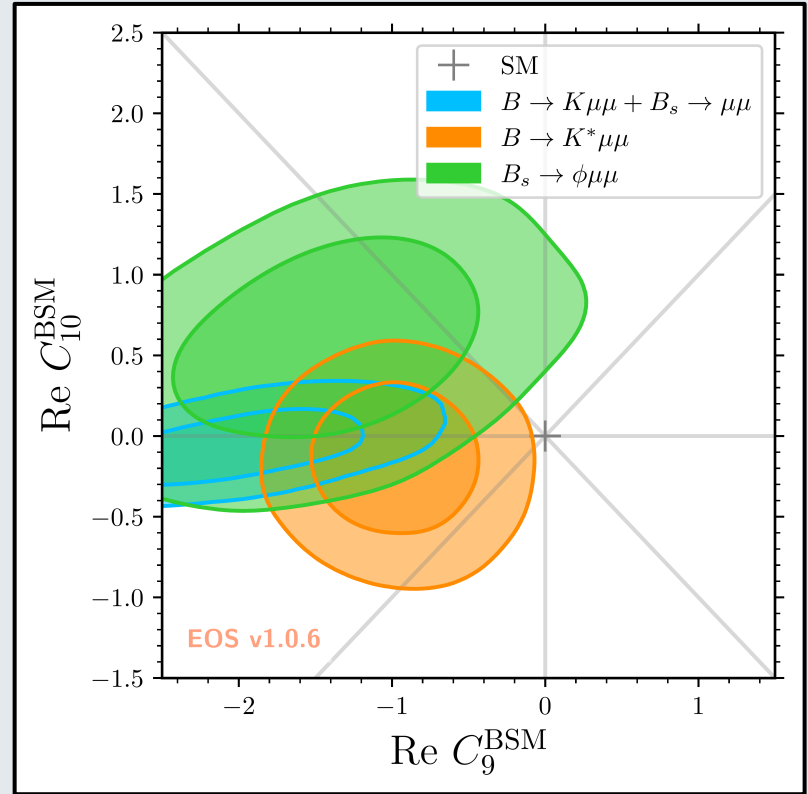


IV. BSM analysis: proof of concept

BSM ‘proof-of-concept’ analysis



- A combined BSM analysis would be **very CPU expensive** (130 correlated, non-Gaussian, nuisance parameters!)
- Fit C_9 and C_{10} **separately** for the three channels:
 - $B \rightarrow K\mu^+\mu^- + B_s \rightarrow \mu^+\mu^-$
 - $B \rightarrow K^*\mu^+\mu^-$
 - $B_s \rightarrow \phi\mu^+\mu^-$

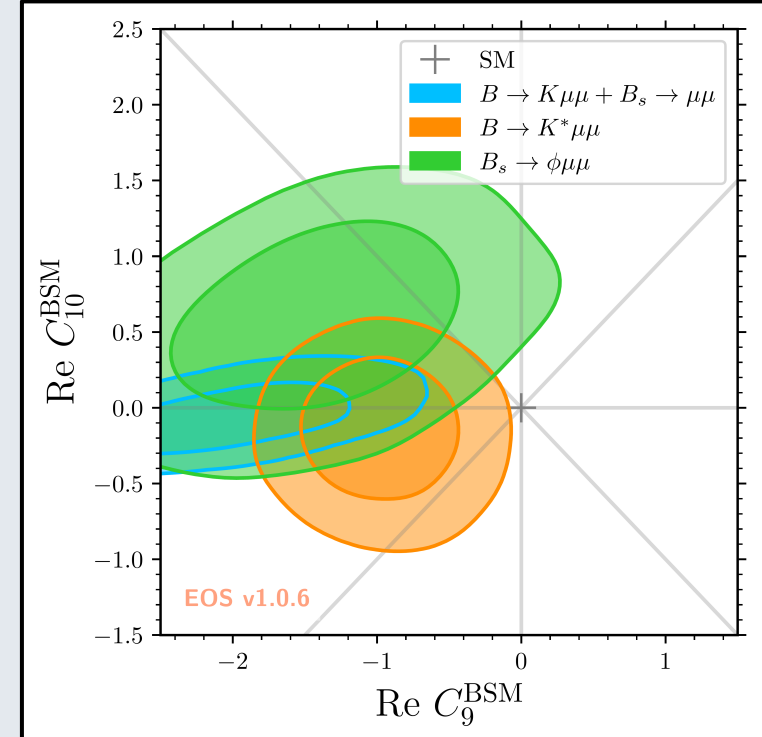
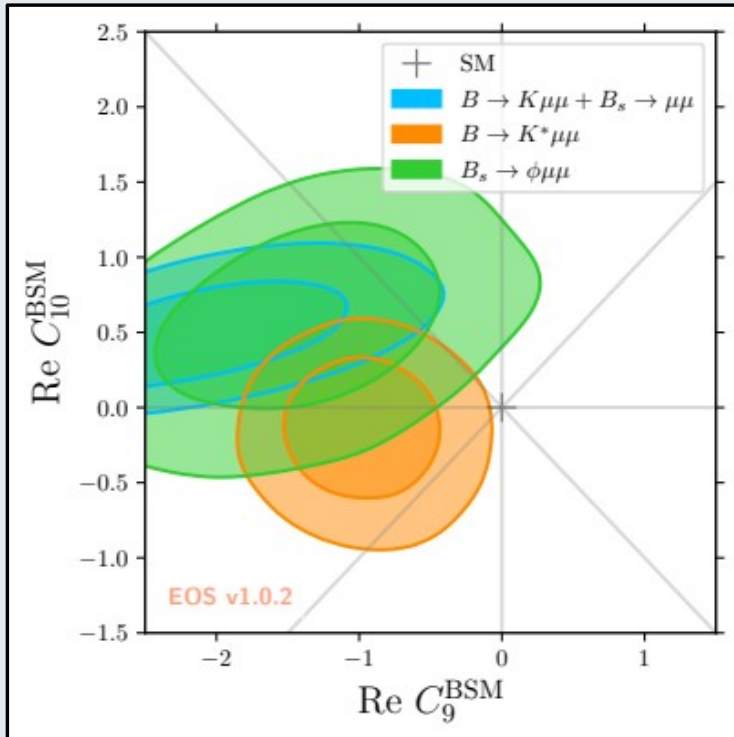


Effect of HPQCD 2022



Accounting for:

- CMS' $B_s \rightarrow \mu^+\mu^-$ measurement [2212.10311] \rightarrow SM-like, $C_{10}^{\text{BSM}} \rightarrow 0$
- HPQCD '22 $B \rightarrow K$ form factors



Conclusion

Discussing BSM models requires a solid understanding of the hadronic physics:

- **Local form factors** uncertainties can be controlled and reduced by using improved dispersive bound and a *appropriate* parametrization
 - This is the first global analysis of $b \rightarrow s$ form factors
 - It is reassuring as it confirms channel-specific analyses...
 - ... and promising as dispersive effects start to be visible
- **Non-local form factors** can also be constrained by theory calculation and experimental measurements

→ In both cases:

- Uncertainties are still large, but controlled by dispersive bounds
- Our approach is systematically improvable

Back-up

